

# Universal Usage of a Video Projector on a Mobile Guide Robot

Ronny Stricker<sup>(✉)</sup>, Steffen Müller, and Horst-Michael Gross

Neuroinformatics and Cognitive Robotics Lab,  
Technische Universität Ilmenau, 98693 Ilmenau, Germany  
ronny.stricker@tu-ilmenau.de  
<http://www.tu-ilmenau.de/neurob>

**Abstract.** In this paper, we present a holistic approach to enable mobile robots using video projection in a situation aware and dynamic way. Therefore, we show how to autonomously detect wall segments that are suitable to be used as projection target in a dynamic environment. We derive several quality measures to score the wall segments found in the local environment and show how these scores can be used by a particle swarm optimization to find the best local projection position for the mobile robot.

**Keywords:** Mobile robot · Video projection · Position optimization

## 1 Introduction

User interaction plays a very important role for mobile service robots. It should be possible to easily use them and to get a real benefit from the offered service. However, current generations of these robots do have some shortcomings in presenting information in an appropriate and easily understandable manner. The idea of using video presenters on a mobile robot states back to the first Star Wars films and can help to improve the intelligibility of the information provided by the robot [1]. This is especially true for our tour robots Konrad and Suse that are used to guide and to tour people around in our multi-story faculty building [2]. In order to increase the acceptance of the tour guide scenario, the robots should not only talk to the user and give information on the on-board display, but also make use of walls next to the exhibit to display information. Since the exhibits can change over time, it will be beneficial if the robot can optimize its position and the wall used for projection depending on the local surroundings and the location of the current audience.

In addition to the problem of finding an appropriate position and wall segment used for projection, we also need to address the problem of projector calibration. As the robot is not usually oriented perpendicular to the wall, the projection will get distorted. This problem increases if the user itself is not oriented perpendicular to the projection wall. Therefore, we show how to implement

two different projection modes that do rectify the image without the need of calibration images. In the first mode, the image is rectified according to the wall used for projection. In the second mode, the image is rectified according to the user position and therefore seams to be floating on the wall.

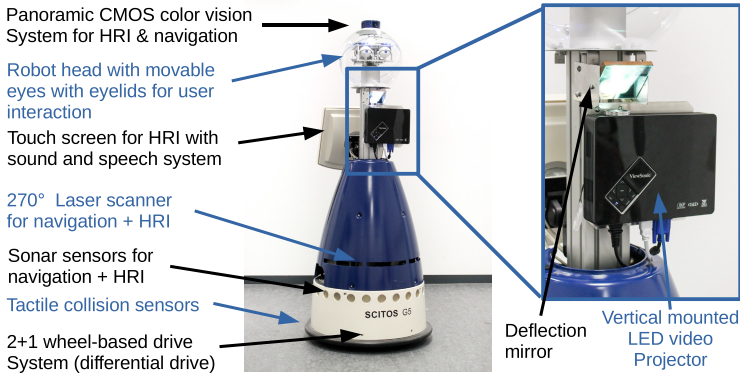


**Fig. 1.** Robot platform with mounted LED video projector and deflection mirror.

Fig. 1 shows the experimental platform used for our research. It is equipped with interaction devices, mainly a touch-display, as well as a couple of additional sensors enabling autonomous navigation and perception of people and obstacles in the robots environment. In addition to this regular setup, the test platform has been equipped with a LED video projector (ViewSonic PLED-W500). The projector is mounted together with a deflection mirror in a vertical position below the robot head to guarantee minimum space requirements. It does deliver 500 lumens of brightness at a maximum power consumption of 120 W, which is of course questionable for the desired field of application. However, current generations of small LED based projectors have already doubled or tripled brightness and can easily replace our projector used for demonstration purpose.

To deal with the different problems arising from the dynamic projector position optimization the paper is structured as follows: After a brief overview of the related work and the presentation of the prerequisites of our work we are giving a detailed overview of our proposed method and the involved score functions in Sec. 4. After the distortion correction has been explained in Sec. 5, we are showing some experiments and finish with a conclusion in Sec. 7.

## 2 Related Work

Several methods can be found, that are dealing with aspects of the problem we have described above. The largest group has been emerged during the last few years and tries to integrate a video projector onto a guide robot. One example is given in [3]. The authors are using a pan and tiltable video projector to display addition information of exhibits onto the wall. Furthermore, the projector is

used to project buttons on the ground, that can be activated by means of the users feet. In [4] a guide robot is used to augment a guiding tour by projecting directly onto different exhibits in order to highlight the parts explained but also to simulate ancient computer models by projecting directly onto a switched off monitor. The authors of [5] are using the humanoid robot NAO to project information on walls in a home environment. However, the robot position as well as the projection surface are predefined in this approach. Two examples of methods combining video projection with gesture detection are given in [6,7].

Since the surfaces used for projection are predefined in all the methods stated above, none of these tries to find an optimal projection surface in the local environment dynamically. Most of the methods do even rely of fixed and predefined robot positions that are aligned perpendicular to the wall.

Current methods for camera based projection calibration do rely on predefined patterns that are displayed during initialization phase [8,9]. Since the robot changes its pose relative to the projection surface once it is moving, a closed loop algorithm, as used by other methods for projection, correction cannot be applied.

### 3 Prerequisites

In order to build and to explain the projector position optimization, we rely on different components that are not in the scope of this paper.

First, we are using MIRA [10] as software framework in order to combine all the different modules in an easy and efficient way. The integrated transformation framework of MIRA enables us to step back and forth between the different coordinate frames (robot frame, map frame, person frame) easily.

Second, we also need to take the user position, view direction and walk direction into account. To reliably track persons in the local environment we are using the probabilistic multi-hypotheses people detection and tracking system developed in our lab over the last eight years [11]. It is based on a 7D Kalman filter that tracks the position, velocity, and upper body orientation of the respective persons assuming an uncertain random acceleration. The tracker processes the detections of different, asynchronous observation modules – namely a 2D laser-based leg detector, a face detector, a motion detector, and an upper-body shape detector. The leg detector in its initial version is based on the boosted classifier approach of [12]. The face detection system utilizes the well-known face detector of Viola & Jones [13]. Finally, we apply an upper body shape detector based on Histograms of Oriented Gradients (HOG) [14]. A detailed description of the person detector and tracker and the tracking results of comparing evaluation studies on different data sets with increasing difficulty is given in [11].

Third, we are relying on mapping and localization algorithms proven to work robust during several years [15]. These algorithms include the generation of a local map (8x8 meters in our application) and covers the local surroundings seen by the robot so far.

## 4 Finding Optimal Projection Surface and Position

Finding an optimal projection position in our eyes falls into two tasks. First, the detection of walls in the local surrounding that are candidates for a projection target. Second, we need to take the user and the robot position into account to score the wall candidates in order to obtain the best projection surface. Three aspects are of importance during scoring. The wall needs to be visible to the user and should show an appropriate distance and view angle. Furthermore, it should be possible to project onto the wall. Therefore, it should show a suitable brightness and color and should not have any dominant structure (no signs or posters should cover the wall). Moreover, the wall should be in range of the projector, which again sets requirements on the distance and angle of the wall. The person visibility and wall structure related demands do not depend on the current robot position, therefore, we do relate to these requirements as *robot position independent score functions* in the remainder of this paper. In turn the other requirements are *robot position dependent*.

Walls in the local surrounding can be very long, the suitability is likely to fluctuate heavily at different positions. Therefore, we break the walls apart by dividing them into different wall segments, that are scored independently. It would be possible to use a real 3d segmentation for this step. However, it would increase the computational complexity a lot and cause only a slight benefit in our scenario since we are not able to pan or tilt the projector. Therefore, we are using wall segment with fixed width (30 cm in our application as a trade of between computational complexity and spacial resolution) and a fixed height of 1.2 meter (1 meter above the ground) during the segmentation phase.

Having a closer look at the requirements and at the application scenario reveals that the overall problem is twofold. The first task is to find the best suited wall segment(s) for the current position of the robot. The second task is more general and comprises finding of the best robot position, so that the best wall segment(s) in the local surrounding can be used for projection (Fig. 2). The second task involves the first one, since we need to evaluate the maximum score for different robot locations and orientations in the local surrounding. Since evaluating all possible robot poses in the local surrounding is way to expensive, we apply a particle swarm optimization (PSO) [16] to find the optimal projection position. Therefore, every particle returns the score of the best segment(s) that can be used for projection from this single position.

The two tasks can be applied directly to our application scenario where we can use the PSO approach to find the best location for augmenting the exhibit presentation.

In the remainder of this section we explain the wall extraction and the different score functions in more detail.

### 4.1 Wall Segment Extraction

For wall extraction we do not rely on a pre-build map, since the public environment is likely to change so that walls can be covered by trolleys, posters or

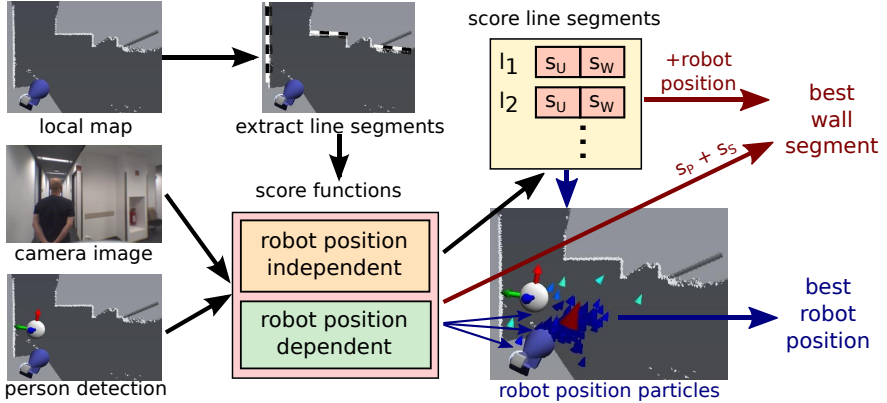


**Fig. 2.** Overview of process to find the best wall segment (red) and robot position (blue). The robot position independent scores need to be computed only once and can be stored with the segment. The robot position dependent scores need to be recomputed every time the robot pose changes. The image at the bottom right shows the result of a PSO with 200 particles with the best particle colored in red.

other obstacles. Therefore, we are using the local map that does contain the local surroundings as seen by the robot so far.

The wall segmentation is performed using a *Random Sample Consensus* (RANSAC) [17] based algorithm for line fitting on all the points marked as obstacle in the local map. The algorithm searches and returns the line hypothesis with the most points supporting the hypothesis. Removing the supporting points (that also determine the start and endpoint of the line) and repeating the process as long as lines with a specified support can be found, results in the extraction of the best  $n$  lines for the local surrounding which correspond to the walls. These lines are split into smaller line segments with a fixed length (30 cm in our application).

## 4.2 Robot Position Independent Cost Functions

The first cost functions to be discussed are independent of the robot’s position and need to be computed only once for every run of the PSO. Please note that we try to use Gaussian score function whenever possible to help the PSO particles to find a gradient if they are far away from the optimum.

**User Dependent Segment Visibility.** To check if a segment is visible to the user. The line of sight between the user (defined by its position  $\mathbf{p}_u$  and its orientation normal  $\mathbf{n}_p$ ) and the segment  $i$  (defined by its position  $\mathbf{p}_{i_1}$  and orientation normal  $\mathbf{n}_{i_1}$ ) is free of obstacles. Therefore, we trace the local map between the points  $\mathbf{p}_u$  and  $\mathbf{p}_{i_1}$  and set the obstacle score  $s_O$  to zero if we found an obstacle and to 1 otherwise. Furthermore, we need to take the visual field of

the user into account. Therefore, we compute the angle between the line of sight and the person orientation normal as  $\alpha_{Segment} = \text{acos}((\mathbf{p}_u - \mathbf{p}_i) \cdot \mathbf{n}_p)$ . Assuming that the visual field of a human is almost  $180^\circ$  with a central field of  $90^\circ$  we are using a spitted Gaussian function  $s_{VF}(l_i) = g_{sp}(\alpha_{Segment}, -\pi/4, \pi/4, 0.35, 0.35)$  that returns 1 for the central field and drops of the almost zero at  $90^\circ$  on each side.

$$g_{sp}(x, lo, up, s_1, s_2) = \begin{cases} \exp(-\frac{(x-lo)^2}{2s_1^2}), & x < lo \\ \exp(-\frac{(x-up)^2}{2s_2^2}), & x > up \\ 1, & lo \leq x \leq up \end{cases} \quad (1)$$

The last of the tree sub scores, is the distance score. We suggest preferring segments with a distance between 1.5 and 4 meter using the split Gaussian  $s_D(l_i) = g_{sp}(\|\mathbf{p}_u - \mathbf{p}_i\|_2, 1.5, 4.0, 1.0, 1.7)$ . Therefore, the resulting score of the user dependent segment visibility  $s_U$  becomes:  $s_U(l_i) = s_O(l_i) \cdot s_{VF}(l_i) \cdot s_D(l_i)$ .

**Projection Suitability.** It is important that the wall segments used for projection purpose are of a bright and uniform color and are clear of obstacles.

Using a calibrated camera we can extract the image regions associated with the single segments and analyze them in terms of color and structure. We project the 3D-world position of the segment edges into the image space and extract the gray-scale image region (Fig. 3). Afterwards, the average image value is derived. This value should not be too close to white, as ceiling light might outshine the projected image, nor should it be too dark or have any extreme color cast. Therefore, we are using a Gaussian function aiming at an average gray value of  $2/3$  of the maximum possible gray value to compute brightness subscore  $s_B(l_i) = \text{Gauss}(\text{Avg}(l_i), \mu = 170, \sigma^2 = 50)$ . The structure of the segment is analyzed by computing the magnitude of the Sobel-filtered image region in x and y direction. Since the segments can become unsuitable for projection even if the magnitude is far away from the maximum value, we use a low threshold for the score function that allows a maximum average gradient magnitude of 40:  $s_G(l_i) = \text{max}(0, 1.0 - \text{AvgMag}(l_i)/40)$ . Thus, the resulting wall projection suitability score gets  $s_W(l_i) = s_B(l_i) \cdot s_G(l_i)$ .

The drawback of this approach is that not all the segments are visible to the camera and that they can be shadowed by persons and thus get wrong score values. To avoid this problem, the module stores a local segment history (same 8x8 meter environment as the local map). If segments are shadowed by persons (details on how to detect shadowing are given in the Sec. 4.3), the suitability score is not updated. The same applies if a segment is currently used for projection, since the projector changes the score of the segment. If the score cannot be obtained, we take the score from a similar segment in the history buffer.

### 4.3 Robot Position Dependent Cost Functions

The second group of cost functions depends on the robot pose and therefore needs to be computed for every single robot pose hypothesis.

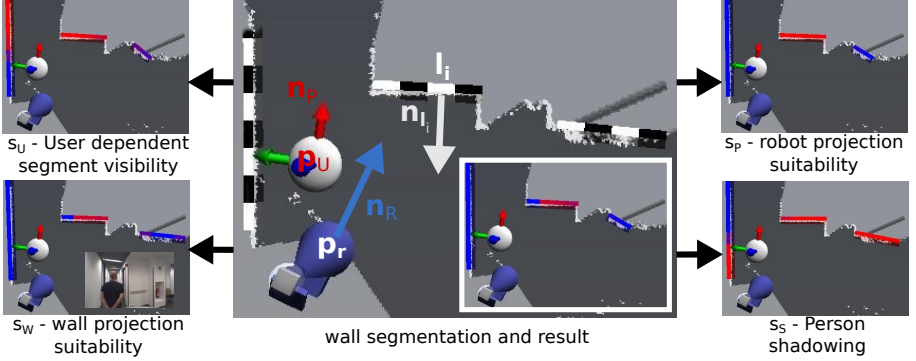


**Fig. 3.** Results of the different score functions for an exemplary situation. The line segments are color coded according to the result of the score functions with blue being the lowest score. Please note that the line segments do vary slightly since the images were recorded consecutively and the RANSAC algorithm varies due to its random nature.

**Robot Projection Suitability.** This cost function is mostly related to the limitations of the video projector and combines three different sub scores. First, similar to the person visibility function, the line of sight between  $\mathbf{p}_r$  and  $\mathbf{p}_i$  needs to be free of obstacles ( $s_O$ ). Second, the projector offers only a limited aperture angle, therefore segments that cannot be covered by the projector need to get a very low score. We compute the angle between segment normal and robot with  $\alpha_{Robot} = \text{acos}((\mathbf{p}_r - \mathbf{p}_{s_i}) \cdot \mathbf{n}_r)$  and combine it with the split Gaussian to match the projector opening angle of  $60^\circ$ :  $s_{PA}(l_i) = g_{sp}(\alpha_{Segment}, -\pi/6, \pi/6, 0.05, 0.05)$ . The last subscore regards the distance between projector and wall. Since the projector has only limited brightness and the focus is fixed, the projector needs to stay within a certain distance range to offer acceptable projections. Therefore, we select the optimum distance to be within 1.4 and 2 meter and let the score drop on both ends:  $s_D(l_i) = g_{sp}(\|\mathbf{p}_r - \mathbf{p}_i\|, 1.4, 2, 0.5, 1.5)$ . Again, the combined score  $s_P$  becomes  $s_P(l_i) = s_O(l_i) \cdot s_{PA}(l_i) \cdot s_D(l_i)$ .

**Person Shadowing.** Segments that, according to the robot position, are shadowed by or next to a person should not be used for projection for two reasons. First, it makes a proper projection impossible if the person is blocking the projected image. Second, a person can be dazzled. Therefore, we penalize segments, when the angle between the line of sights of the segment and all person hypothesis  $p_i$  is too low:  $\alpha_{min} = \min_{\forall p_i}(\text{acos}((\mathbf{p}_r - \mathbf{p}_i) \cdot (\mathbf{p}_r - \mathbf{l}_i)))$   
 $s_S(l_i) = 1.0 - \text{Gauss}(\alpha_{min}, \mu = 0, \sigma^2 = 0.1)$ .

#### 4.4 Selecting the Best Wall Segment for Projection

To find the best wall segment for a given robot position  $\mathbf{p}_r$  and orientation  $\mathbf{n}_r$  the robot position dependent ( $s_P, s_S$ ) and independent score functions ( $s_U, s_W$ ) have

to be computed. Afterwards, the scores of the different functions are multiplied for every segment independently. We use multiplication for this step since the different constraints cannot compensate each other. Segments that are below a certain threshold will be rejected and removed from the set of segments. In a final step, adjacent wall segments get merged, whereby the score of the new segment is the sum of its sub-segments. This guarantees that large segments are preferred. Finally, the segment with the highest score is returned as the best segment for projection for the current robot and user positions.

## 5 Projection Correction

As already stated above, the projected image gets distorted if the projector is not aligned perpendicular to the projection wall. Fortunately, the distortion correction is relatively easy for unbowed, straight walls if the angle between the projector and the wall is known.

Since the position and orientation of the wall segment used for projection is known from the position optimization, we can compute coordinates of the rectified image in the image space by means of vector geometry (Fig. 4).

Once we have obtained the image coordinates of the distorted and the rectified image, we can compute a point correspondence matrix (homography matrix) to distort the input image for the projector so that it is displayed correctly on the wall segment.

### 5.1 Wall Rectified Projection

Knowing the video projector pose  $\mathbf{p}$  and its aperture angle, we can compute the intersection points of the four image corners ( $lu, ru, ll, rl$ ) with the plane  $H$  defined by the target wall segment  $S$ . Afterwards we transform these 3D coordinates ( $lu_{3D}, ru_{3D}, ll_{3D}, rl_{3D}$ ) on the plane to obtain 2D coordinates ( $lu_H, ru_H, ll_H, rl_H$ ) of the beamer edge points. After the  $x$  coordinates of these points have been adapted to stay within the region defined by the desired wall segment  $l_i$ , we compute the maximum rectangle with the aspect ratio defined by the projector ( $lu_{max'}, ru_{max'}, ll_{max'}, rl_{max}'$ ). These points are transformed back to 3D coordinates and projected back into the beamer frame to get the points  $lu_{max}, ru_{max}, ll_{max}$  and  $rl_{max}$ . Together with the points  $lu, ru, ll$  and  $rl$  they are defining point correspondences, which are used to compute the planar homography matrix that defines the image distortion. The resulting projection rectifies the image according to a perpendicular observer position.

### 5.2 User Adaptive Projection

An alternative rectification takes the position of the observer into account and rectifies the image in order to make it appear perpendicular to the axis of view. Therefore, we define a plane  $V_o$  that is 10 cm in front of the observer in direction of the segment center  $c$ . This plane is oriented perpendicular to the observer view



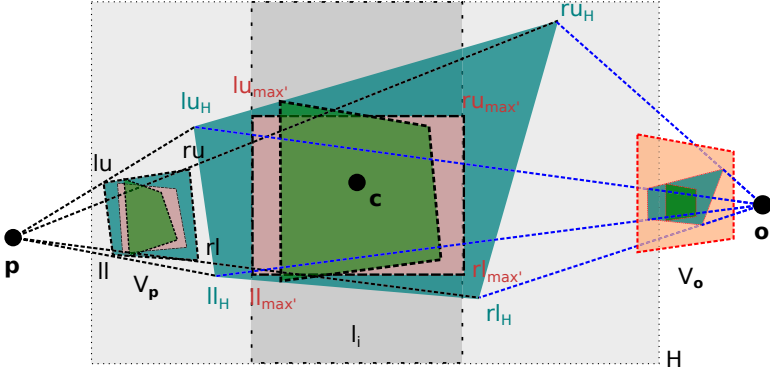


**Fig. 4.** Illustration of the image rectification process. The projector edge coordinates are projected into the wall or observer coordinate system. Afterwards, they are rectified and projected back into the projector frame.

direction and has the normal vector  $c-o$ . In contrast to the observer independent approach, the 3D coordinates  $lu_{3D}, ru_{3D}, ll_{3D}, rl_{3D}$  are projected onto this plane  $V_o$  using the vectors from the corner coordinates to the observer. Therefore, the maximum rectangle is computed on the observer plane  $V_o$  before the coordinates are projected back onto the wall plane and from there to the projector space in order to yield the homography matrix.

## 6 Experiments

Experiments have been conducted with the actual robot platform in our faculty building and using a robot simulator.

We have tested the extraction of suitable wall segments and the projection rectification for different exhibits and situations in our lab. Results for two situations are given in Fig. 6. For every location the local surrounding (8x8 m) of the robot and the user position was taken into account. The algorithm was able to generate a rectified projection on wall segments that are of good visibility to the user. However, the position optimization tends to generate positions with acute projection angle as these positions are good in terms of user visibility and maximum projection distance. If maximum projector brightness is an issue, we recommend integrating an additional module for rating the robot to wall angle.

An analysis of the runtime of the different algorithm steps on the robot platform running an Intel Core i7-3612QM was conducted. As a result, segment detection (18.6 ms) and computation of the robot position independent modules (6.1 ms) is required only once for every new person detection. It has to be noted, that the quality of the optimization highly depends on a proper line extraction of the RANSAC algorithm. Although, it fluctuates a bit, it has proven to work well enough for wall segments with a minimum length of 60 cm. The robot position dependent modules need to be computed for every new particle hypotheses. During our tests, we configured the PSO to use 500 particles and

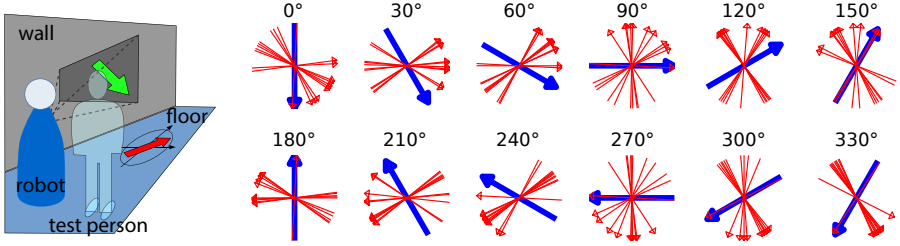


**Fig. 5.** *left:* Set up of the projection experiment. *right:* interpreted directions of the test persons (red) for displayed arrow (blue) and for unrectified projection.

to stop optimization if the score improvement is lower than 5 percent for 5 generations. This leads to an average of 7 iterations in order to obtain a stable optimum position and requires 35.1 ms of run time on average.

The update rate of the goal position optimization is limited to 10 Hz, which is the update rate of the laser range finder and thus the frequency of the person detection. Furthermore, the person detection accuracy does fluctuate over time requiring smoothing of the person pose as small changes in the person pose do have a high impact on the person specific projection. Therefore, the person dependent projection is always a bit behind if the person is moving fast. However, people are unlikely to move very fast during the presentation of an exhibit.

In order to test the benefit of the projection rectification, we have set up the experiment given in Fig. 5. The robot was located 50 cm in front of a wall, facing the wall at an acute angle causing strong image distortions. We have asked 11 test persons to stand 1 meter next to the robot and to view the images projected by the robot with three different methods: (a) no correction, (b) wall rectified correction, (c) user adaptive projection. First of all, we showed them a video with the different projection methods and ask which one was most comfortable to view. Since only one person prefers the uncorrected projection, image rectification can improve the presentation quality. However, the type of preferred correction is person dependent ( 4 votes for (b) and 6 votes for (c)) and should be inquired at the beginning of a tour. In the second stage we examined, how the different projections affect the interpretation of direction arrows that might point to the next exhibit. Therefore, we consecutively presented an arrow rotated randomly between  $0^\circ$  and  $360^\circ$  (with  $30^\circ$  increment) on the projection area and asked the test persons to interpret the shown arrow in the floor coordinate system (Fig. 5). Although, the average deviation of subjective angle perception decreases from  $62.7^\circ$  for (a) to  $46.81^\circ$  (b) and  $49.09^\circ$  (b) it has to be noted, that the person specific preference is more important than the chosen rectification method. Therefore, the diagrams for (b) and (c) are almost identical to the one given in Fig. 5. It seems that the viewing angle of the test person to the arrow position on the wall has more influence than the actual type of projection and therefore should be considered while generating instruction arrows.



**Fig. 6.** Example image for the wall segment extraction and projection rectification. left: unmodified and distorted projection. middle: projection after segment extraction and rectification. right: direction information displayed on the wall.

## 7 Conclusion and Future Work

This paper describes a new method that takes the user position into account in order to dynamically extract wall segments that are suitable for video projection. Furthermore, we show how to embed the scoring of the wall segment extraction into an PSO framework in order to obtain the best projection position for the robot in the local surrounding.

Continuing our work, we are currently working on the integration of the robot position scoring into the local motion planning algorithm of the robot. We are using a dynamic window approach (DWA) [18] for motion planning, that samples the possible velocity commands of the robot within a certain prediction time window and scores them by different navigation objectives (e.g. Distance to obstacles, follow a path, follow a person with a given distance,..) [19,20]. We already extended this approach to also score the motion trajectories in terms of projection suitability. First experiments already show promising results as the average projection score during driving can be increased significantly. This allows the robot to improve the experience during a guided tour by projection information (e.g. directions) onto walls during driving.

Furthermore, the work presented so far is designed to work with one user only. Therefore, in future we want to find out if and how the method can be extended to work with multiple users at a time.

## References

1. Kwon, E., Kim, G.J.: Humanoid robot vs. projector robot: exploring an indirect approach to human robot interaction. In: Proc of 5th ACM/IEEE International Conference on Human-Robot Interaction (HRI), pp. 157–158, March 2010
2. Stricker, R., Müller, S., Einhorn, E., Schrtter, C., Volkhardt, M., Debes, K., Gross, H.-M.: Interactive mobile robots guiding visitors in a university building. In: Proc. 21st IEEE Int. Symposium on Robot and Human Interactive Communication (Ro-Man), Paris, France, pp. 695–700, September 2012
3. Sasai, T., Takahashi, Y., Kotani, M., Nakamura, A.: Development of a guide robot interacting with the user using information projection basic system. In: International Conference on Mechatronics and Automation, pp. 1297–1302, August 2011
4. Donner, M., Himstedt, M., Hellbach, S., Boehme, H.-J.: Awakening history: preparing a museum tour guide robot for augmenting exhibits. In: Proc. European Conference on Mobile Robots (ECMR), pp. 337–342, September 2013

5. Panek, P., Edelmayer, G., Mayer, P., Beck, C., Rauhala, M.: User acceptance of a mobile LED projector on a socially assistive robot. In: Wichert, R., Eberhardt, B. (eds.) *Ambient Assisted Living. ATSC*, vol. 2, pp. 77–92. Springer, Heidelberg (2012)
6. Choi, S.-W., Kim, W.-J., Lee, C.H.: Interactive display robot: projector robot with natural user interface. In: *Proceedings of the 8th ACM/IEEE International Conference on Human-Robot Interaction (HRI 2013)*, pp. 109–110. IEEE Press, Piscataway (2013)
7. Ishii, K., Zhao, S., Inami, M., Igarashi, T., Imai, M.: Designing laser gesture interface for robot control. In: Gross, T., Gulliksen, J., Kotzé, P., Oestreicher, L., Palanque, P., Prates, R.O., Winckler, M. (eds.) *INTERACT 2009. LNCS*, vol. 5727, pp. 479–492. Springer, Heidelberg (2009)
8. Moreno, D., Taubin, G.: Simple, accurate, and robust projector-camera calibration. In: *Second International Conference on 3D Imaging, Modeling, Processing, Visualization and Transmission (3DIMPVT)*, pp. 464–471, October 2012
9. Audet, S., Okutomi, M.: A user-friendly method to geometrically calibrate projector-camera systems. In: *Conference on Computer Vision and Pattern Recognition Workshops. IEEE Computer Society*, pp. 47–54, June 2009
10. Einhorn, E., Langner, T., Stricker, R., Martin, Ch., Gross, H.-M.: MIRA - middleware for robotic applications. In: *Proc. IEEE/RSJ Int. Conf. on Intelligent Robots and Systems (IROS 2012)*, Vilamoura, Portugal, pp. 2591–2598, October 2012
11. Volkhardt, M., Weinrich, Ch., Gross, H.-M.: Multi-modal people tracking on a mobile companion robot. In: *Proc. 6th European Conference on Mobile Robots (ECMR 2013)*, Barcelona, Spain, pp. 288–293, September 2013
12. Arras, K.O., Mozos, O.M., Burgard, W.: Using boosted features for the detection of people in 2d range data. In: *IEEE International Conference on Robotics and Automation 2007*, pp. 3402–3407 (2007)
13. Viola, P., Jones, M.: Rapid object detection using a boosted cascade of simple features. In: *Proc. of the IEEE Computer Society Conference on Computer Vision and Pattern Recognition (CVPR)*, vol. 1, pp. 511–518 (2001)
14. Weinrich, Ch., Vollmer, Ch., Gross, H.-M.: Estimation of human upper body orientation for mobile robotics using an SVM decision tree on monocular images. In: *Proc. IEEE/RSJ Int. Conf. on Intelligent Robots and Systems (IROS 2012)*, Vilamoura, Portugal, pp. 2147–2152, October 2012
15. ROREAS project. [www.roreas.org](http://www.roreas.org)
16. Kennedy, J., Eberhart, R.: Particle swarm optimization. In: *IEEE International Conference on Neural Networks*, vol. 4, pp. 1942–1948, November/December 1995
17. Fischler, M.A., Bolles, R.C.: Random sample consensus: a paradigm for model fitting with applications to image analysis and automated cartography. *Commun. ACM* **24**(6), 381–395 (1981)
18. Fox, D., Burgard, W., Thrun, S.: The dynamic window approach to collision avoidance. *IEEE Robotics & Automation Magazine* **4**(1), 23–33 (1997)
19. Gross, H.-M., Debes, K., Einhorn, E., Müller, St., Scheidig, A., Weinrich, Ch., Bley, A., Martin, Ch.: Mobile robotic rehabilitation assistant for walking and orientation training of stroke patients: a report on work in progress. In: *Proc. IEEE Int. Conf. on Systems, Man, and Cybernetics (SMC 2014)*, San Diego, USA, pp. 1880–1887, October 2014
20. Einhorn, E., Langner, T.: Pilot - modular robot navigation for real-world-applications. In: *Proc. 55th Int. Scientific Colloquium*, Ilmenau, Germany, pp. 382–393. Verlag ISLE 2010